Original Article

Focused Ultrasound Sonications of Tumor Model in Head Phantom under MRI Monitoring: Effect of Skull Obstruction on Focal Heating

Anastasia Antoniou[1], Antreas Chrysanthou[2], Leonidas Georgiou[2], Antonis Christofi[2], Yiannis Roussakis[3], Cleanthis Ioannides[2], Kyriakos Spanoudes[4,5], Jufeng Zhao[6], Liyang Yu[6], Christakis Damianou[1,6]

[1]Department of Electrical Engineering, Computer Engineering, and Informatics, Cyprus University of Technology, Departments of [2]Diagnostic and Interventional Radiology and [3]Radiation Oncology, German Medical Institute, Limassol, [4]Department of Veterinary Medicine, University of Nicosia School of Veterinary Medicine, [5]VET EX MACHINA Limited, Nicosia, Cyprus, [6]Department of Electronics and Information Engineering, Hangzhou Dianzi University, Hangzhou, Zhejiang, China

Abstract

Purpose: This study presents the outcomes of a series of magnetic resonance imaging (MRI)-guided focused ultrasound (MRgFUS) sonications performed on an anatomically accurate head phantom with an embedded tumor simulator to evaluate the effectiveness of partial and complete tumor ablation with obstruction from thin polymer skull mimics. **Materials and Methods:** The tumor simulator was subjected to single and grid sonications using a single-element concave transducer integrated with an MRI-compatible focused ultrasound (FUS) robotic system. All experiments were carried out in a high-field MRI scanner utilizing proton resonance frequency thermometry and T2-weighted (T2-W) turbo spin echo (TSE) imaging to evaluate the induced thermal effects. FUS transmission through 1-mm thick three-dimensional-printed polymer skull mimics was compared to unobstructed sonication through a circular aperture in the skull model. **Results:** T2-W TSE imaging demonstrated sharp contrast between the tumor and hyperintense FUS lesions. Complete tumor coverage was achieved through robotic-assisted grid ablation without a skull mimic, as well as with a 1-mm resin skull mimic intervening in the beam. With the lowest attenuation among tested polymers, the resin skull resulted in approximately a 20% reduction in focal temperature change compared to unobstructed sonication, yet still facilitated sharp beam focusing, raising the tumor temperature to ablative levels. **Conclusions:** The study provides preliminary evidence for the potential application of a thin biocompatible implant to temporarily replace a skull portion facilitating MRgFUS ablation of inoperable tumors using a single-element transducer. The tumor-embedded head phantom was proven effective for testing MRgFUS oncological protocols and equipment.

Keywords: Focused ultrasound, head phantom, magnetic resonance thermometry, robotic system, T2-weighted turbo spin echo imaging, tumor simulator

Received on: 18-10-2024 **Review completed on:** 02-01-2025 **Accepted on:** 03-01-2025 **Published on:** 07-03-2025

Introduction

A diverse range of preclinical *ex vivo* models for evaluating thermal therapy modalities, such as focused ultrasound (FUS), before *in vivo* studies is detailed in the literature, which helps reduce the reliance on animal testing.[1-3] *Ex vivo* tumor models play a crucial role in early oncology research by providing a cost-effective alternative to traditional animal models. In this context, gel-based tumor-bearing tissue mimicking phantoms (TMPs) have emerged as a valuable testing tool minimizing the need for animal tissue.[1-3]

In response to the need to minimize the use of animal tissues, recent studies have focused on the development and application of tumor-bearing TMPs that contain no animal-derived materials in thermal ablation research.[4-9] Notably, there has been a focus on tumor phantoms specifically for radiofrequency ablation (RFA) and microwave ablation (MWA), largely driven by their extensive application in the treatment of hepatocellular carcinoma.

Zhong *et al*.[4] proposed a tumor-bearing phantom model for thermal ablation, featuring a 3-cm spherical tumor mimic

Access this article online

Quick Response Code:

Website: www.jmp.org.in

DOI: 10.4103/jmp.jmp_177_24

Address for correspondence: Prof. Christakis Damianou, Department of Electrical Engineering, Computer Engineering and Informatics, Cyprus University of Technology, 30 Archbishop Kyprianou Street, Limassol 3036, Cyprus.
E-mail: christakis.damianou@cut.ac.cy

How to cite this article: Antoniou A, Chrysanthou A, Georgiou L, Christofi A, Roussakis Y, Ioannides C, *et al*. Focused ultrasound sonications of tumor model in head phantom under MRI monitoring: Effect of skull obstruction on focal heating. J Med Phys 2025;50:38-45.

embedded in a cubic gel phantom. Both sections were made of polyacrylic acid (PAA) infused with thermochromic ink, while the tumor further included imaging contrast agents. This phantom exhibited a permanent color change at 60°C, enabling clear visualization of the ablation area following ultrasound-guided MWA. In contrast, Zhou *et al*.[5] used a polyacrylamide-based thermochromic tumor phantom, where both the tumor and surrounding tissue were hypoechoic in B-mode imaging, with the tumor only distinguishable by its hyperechoic margins. The potential of breast cancer MWA ablation with three different antenna types was also investigated using fiber optic thermometry on a nonthermochromic phantom.[6] Spherical tumor mimics measuring 1.0 and 1.5 cm in diameter were made from agarose, sodium chloride, and ethanol, while healthy breast tissue was simulated with a mixture of agarose, detergent and oil.[6]

Regarding RFA, two-section cylindrical phantoms were developed to investigate the effect of background tissue thermal conductivity on heating.[7] The inner compartment, representing a tumor, contained a 0.25% agar solution, while the surrounding layer consisted of 5% agar, with its thermal conductivity adjusted by adding a fat-saturated oil-based solute. Fluoroptic thermometry indicated that lower thermal conductivity significantly increased radiofrequency (RF)-induced temperatures within the tumor.[7] In a different approach, Kim and Lee[8] used magnetic resonance (MR) thermometry to explore nanoparticle-mediated RF heating in a two-compartment CuSO4-doped agar phantom, where the inclusion of Fe_3O_4 nanoparticles in the tumor significantly enhanced heat retention. Kaczmarek *et al*.[9] employed a similar tumor model composed of agar and iron oxide nanoparticles, encircled by softer pure agar to mimic healthy tissue, to examine the heating effects of a newly proposed sono-magnetic therapeutic approach.

FUS studies have utilized a variety of phantoms, ranging from simple models to advanced anatomically accurate ones,[10-12] though only a limited number incorporated tumor models. In a recent study,[13] an agar-based phantom was developed for MR-guided FUS (MRgFUS) evaluations, where the tumor was modeled with silica-enhanced agar, contrasting with the surrounding pure agar. The inclusion of silica enhanced tumor visibility in MR imaging (MRI) and heat accumulation in the tumor, as demonstrated by MR thermometry.[13] Building on prior research, a subsequent study[14] proposed a more complex phantom composed of PAA and agar solutions infused with MRI contrast agents and bovine serum albumin (BSA). The phantom model was developed in two versions: a transparent 2-cm (in diameter) agar/PAA tumor embedded centrically in either an opaque cubic block of pure agar or a transparent agar/PAA gel. Both models demonstrated strong MRI contrast between their compartments and allowed real-time visualization of FUS ablation. This was evidenced by a visible color change from BSA coagulation at 55°C, further confirmed by MR thermometry in a 3T MRI scanner, along with significant changes in T2 relaxation properties.[14]

Leveraging findings from previous phantom studies on MRgFUS, the current study employed an anatomically accurate head phantom with an integrated tumor simulator to assess the effectiveness of various MRgFUS protocols aiming for partial and complete tumor ablation. This involved subjecting the tumor simulator to a series of single and grid sonications using a single-element concave transducer integrated with an MRI-compatible FUS robotic system. All sonications were executed in a high-field MRI scanner, where the thermal effects were assessed using thermometry and high-resolution imaging. The tumor was first sonicated through a circular opening in the skull model, followed by sonications performed through 1-mm thick polymer skull mimics. The exploration of sonication through thin skull mimics is driven by the potential to facilitate FUS ablation of inoperable brain tumors with a single-element concave transducer. This approach involves temporarily excising a small section of the skull and replacing it with a thin, biocompatible implant to overcome the limitations of MRgFUS ablation through an intact skull.

Materials and Methods

Head phantom design

The head phantom features a precise skull replica, generated by extracting anatomical models from computed tomography scans of a healthy volunteer.[11] These were postprocessed to isolate the bone and three-dimensional (3D) printed using acrylonitrile butadiene styrene thermoplastic (F270 FDM printer, Stratasys, Minnesota, USA), as previously documented.[11]

For the purpose of the current study, a circular section was removed from the skull model (referred to as the skull mimic) to create an aperture of approximately 28 cm². This modification allowed tumor sonication with or without skull interference, enabling the use of skull mimics made from various 3D-printable polymers to assess their impact on energy deposition to the target. Specifically, three solid skull mimics, each with a uniform thickness of 1 mm, were 3D printed using: Resin (Photon M3 Max SLA printer, Anycubic, China), acrylonitrile styrene acrylate (ASA) (F270 FDM printer, Stratasys, Minnesota, USA), and thermoplastic polyurethane (TPU) (3 Extended FDM printer, Ultimaker, Utrecht, Netherlands). Notably, selection of the specific thickness was guided by findings from a previous phantom study,[15] which demonstrated that 1-mm thick 3D-printed resin samples provide an efficient acoustic window for delivering FUS and heating tissue mimicking material to ablative levels. It is important to note that this previous study assessed induced heating effects using thermometry, whereas the current study employs high-resolution conventional MRI for this purpose.

The skull model was filled with a brain tissue-mimicking material containing a tumor mimic, both made from agar gels. The method involved solidifying an aqueous solution of 6% weight per volume (w/v) agar (Merck KGaA, Darmstadt, Germany) and 4% w/v silica (Sigma-Aldrich, Missouri, USA)

in a releasable mold to create a spherical tumor model, which was then embedded in the normal tissue phantom while in a liquid state. A solution of 6% w/v agar was used to form the healthy tissue compartment. These material concentrations were based on a prior study[13] demonstrating that they yield tissue-like properties and excellent contrast between normal tissue and tumor compartments in MRI, while also enabling the monitoring of FUS ablation protocols via MR thermometry. The final phantom was left to fully gel overnight. The step-by-step procedure for preparing a homogeneous agar-based solution, along with the timing for adding various inclusions, is detailed elsewhere.[16,17]

For each sonication protocol tested, the tumor mimic was embedded at a specific distance from the circular opening on the skull model. Therefore, different phantoms were developed to position the tumor center at depths ranging from 3.5 to 7 cm, facilitating a comprehensive assessment of targeting efficacy across both shallow and deep phantom layers. In each case, a tumor diameter of either 2 or 3 cm was selected.

Experimental setup in MRI

The experimental setup for phantom sonications is illustrated in Figure 1. An existing robotic device[18] was positioned on the bed of a 3T MRI scanner (Magnetom Vida, Siemens Healthineers, Erlangen, Germany). The head phantom was securely held in place above the area where the transducer operates using a dedicated holder, as shown in Figure 1a. A plastic holder was used to position an 18-channel RF coil (Ultraflex small coil, Siemens Healthineers) above the phantom, ensuring stability and proper alignment for imaging. Figure 1b is a T2-W TSE axial image illustrating the arrangement of the head phantom in relation to the transducer, which aligns with the circular acoustic opening of the skull model. This visualization also enabled measuring the distance from the transducer to the tumor center, ensuring accurate targeting. The sequence parameters are detailed in Table 1.

In this study, while the employed robotic device supports movement along three linear axes and rotation around a central axis where the transducer is mounted,[18] only the two horizontal degrees of freedom were utilized. Single-element concave ultrasonic transducers operating at 1.1 MHz were integrated into the device. Two transducer options were available: a larger one with a 90 mm diameter and a 100 mm radius of curvature (Zibo Yuhai Electronic Ceramic Co., Shandong, China) and a smaller transducer with a 50 mm diameter and an 80 mm radius of curvature (Piezo Hannas, Wuhan, China), allowing for targeting across the entire depth of the phantom. The former had an efficiency of 30%, while the latter had an efficiency of 32%.

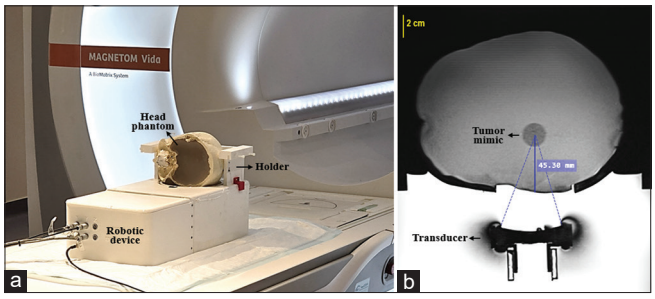

Figure 1: (a) Photo of the basic setup components arranged in the MRI setting. (b) T2-weighted turbo spin echo axial image of the head phantom, with the transducer's focal spot adjusted at the tumor center

Sonication protocols and data acquisition

Single sonications were initially performed targeting the tumor mimic, with variations in power and duration to assess their impact on lesion dimensions and targeting accuracy. Subsequently, grid sonications were conducted to evaluate the feasibility of covering the entire tumor mimic through transducer motion, utilizing the robotic device. Planning for these sonications was performed using the accompanying MRgFUS software,[19] based on preoperative MR images of the experimental setup.

The applied focal intensities ranged from approximately 1800 to 6400 W/cm², with exposure times varying from 20 to 60 s. Focal depths (FDs) of 3.5–7 cm were tested, each using the appropriate phantom with the tumor mimic embedded at the corresponding depth, as explained previously. Depending on the FD, either the smaller (80 mm) or larger (100 mm) radius of curvature transducer was employed. Identical sonications were conducted in an unobstructed field (i.e., without skull interference) and individually across the three 1-mm thick skull mimics, each fixed at the corresponding aperture.

MRI monitoring of thermal effects

The thermal effects resulting from single and grid sonications on the phantom were assessed through MRI techniques, utilizing the available MRgFUS software.[19] Real-time temperature changes were monitored through fast low angle shot (FLASH)-based thermometry, while T2-weighted (T2-W) turbo spin echo (TSE) imaging was utilized to confirm the formation of lesions by detecting changes in signal intensity. A summary of the relevant sequence parameters is provided

Table 1: Employed sequence parameters for T2-weighted turbo spin echo and fast low angle shot imaging

Sequence parameters	T2-W TSE	FLASH
TR (ms)	5000	25
TE (ms)	52	10
FA (°)	110	30
NEX	1	1
FOV (mm²)	260×260	280×280
ST (mm)	3	6
Matrix size	256×256	96×96
ETL	30	1

TR: Repetition time, TE: Echo time, FA: Flip angle, NEX: Number of averages, FOV: Field of view, ST: Slice thickness, ETL: Echo train length, T2-W: T2-weighted, TSE: Turbo spin echo, FLASH: Fast low angle shot

in Table 1. The software employs the Proton Resonance Frequency shift method[20,21] for thermometry, generating thermal maps and simulating areas of necrosis, which are then overlaid on magnitude images of the region of interest in the subject. Thermometry was performed with an acquisition time of 2.4 s per FLASH image.

Results

Figure 2 displays typical thermal maps obtained from high-power exposure targeting the tumor mimic without skull obstruction, using 120 W acoustic power (focal intensity of 6397 W/cm^2) for 40 s, at a FD of 70 mm, along with the corresponding focal temperature evolution. Notably, the large radius of curvature (100 mm) transducer was employed to achieve focusing at this depth.

An indicative example of the characteristic appearance of thermal lesions in the proposed phantom is illustrated in Figure 3. In this case, an acoustic power of 105 W (focal intensity of 5597 W/cm^2) was applied to a 3-cm tumor mimic for 30 s at a FD of 50 mm, again using the large radius of curvature (100 mm) transducer, without skull interference. The resulting lesion exhibited significantly increased intensity and well-defined borders on post sonication T2-W TSE images. Note that in this case, the right lower part of the tumor was intentionally selected as the target during planning on reference coronal images.

Table 2 summarizes thermometry outcomes on the influence of incorporating skull mimics into the beam path on heat accumulation and resulting temperatures within the tumor. Specifically, it compares the maximum temperature and relevant change from a baseline of 19°C after sonication at 80 W for 30 s (FD of 35 mm) using the small radius of curvature (80 mm) transducer, between the unobstructed and skull-obstructed conditions. With this transducer, which has a focal beam area of 4.4 mm^2 (approximately twice that of the larger transducer), 80 W corresponds to a focal intensity of 1838 W/cm^2. In addition, the table includes attenuation coefficient values for the various polymers, which were sourced from prior literature,[22,23] highlighting their impact on FUS energy transmission. Note that since the resin skull had the least influence on focal temperature increase (20% lower increase compared to unobstructed sonication), allowing the generation of ablative temperatures in the tumor, it was selected for use in subsequent experiments.

Further results on tumor ablation without a skull mimic are shown in Figure 4a, which shows a series of postsonication T2-W TSE images of the phantom. In this experiment, a 2-cm diameter tumor was exposed to increasing ultrasonic energy using the smaller radius of curvature (80 mm) transducer at a FD of 45 mm. Note that increasing the ultrasonic energy produced lesions of progressively larger dimensions. Figure 4b illustrates the thermal profile recorded for the highest applied energy of 2400 J (80 W for 30 s), demonstrating a maximum temperature of 73.6°C (ΔT = 54.6°C). For comparison, Figure 4c presents the corresponding T2-W TSE image obtained after sonication using the same parameters but with the resin skull intervening in the beam path. The corresponding peak temperature recorded was 60.7°C (ΔT = 41.7°C), resulting in the formation of a thin, cigar-shaped thermal lesion.

Figure 5 presents the outcomes of a 3 × 3 grid sonication (5-mm step) conducted on a 2-cm tumor mimic using the same transducer, without skull interference. An acoustic power of 80 W (1838 W/cm^2) was applied to each grid point for 60 s, leaving a 60-s cooling time (FD of 35 mm). As shown in Figure 5a, the planned sonication pattern is overlaid on a FLASH image of the phantom, while Figure 5b shows the time series of focal temperature changes for all nine sonication points. The simulated necrosis map in Figure 5c aligns well with the lesion visualized on postsonication T2-W TSE images in Figure 5d, indicating full coverage of the tumor. The sagittal

Table 2: Maximum focal temperature (T_{max}) and corresponding temperature change (ΔT) from sonication at 80 W for 30 s at a FD of 35 mm in the presence of the different 1-mm thick skull mimics, along with their attenuation coefficient, compared to unobstructed sonication (no skull mimic)

Skull mimic	T_{max} (°C)	ΔT (°C)	Attenuation (dB/cm-MHz)
Resin	69.7	50.7	4.2±0.1[23]
ASA	25.9	6.9	15.2±1.6[22]
TPU	21.3	2.3	23.1±2.8[22]
No skull mimic	84.1	65.1	N/A

N/A: Not available, ASA: Acrylonitrile styrene, TPU: Thermoplastic polyurethane

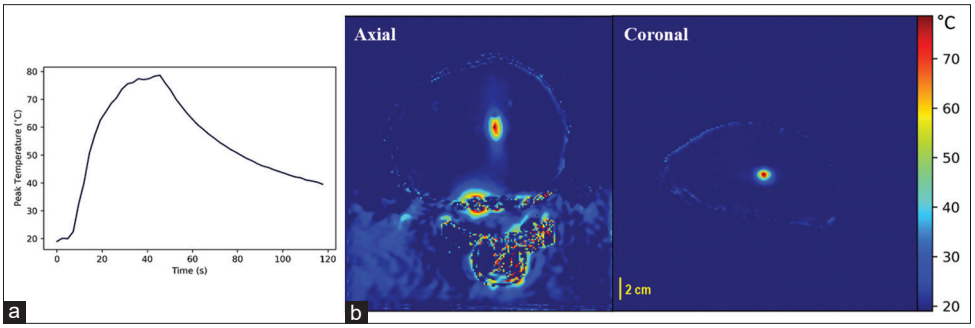

Figure 2: (a) Focal temperature profile during and after a 40-s sonication at 120 W (6397 W/cm^2). (b) Corresponding thermal maps showing temperature distribution within the tumor

and coronal images show the formed overlapping lesion in planes parallel and perpendicular to the beam, respectively, confirming that the tumor mimic was thoroughly treated while minimizing off-target heating. The corresponding thermal profile and a T2-W TSE image of the phantom following a similar sonication through the resin skull mimic are shown in Figure 6.

Discussion

This study builds upon prior research that developed realistic head models and used thermometry to evaluate the effectiveness of FUS ablation through the skull,[11,15,23] along with studies that tested FUS oncological protocols using nonanatomically accurate tumor models.[13,14] By integrating these approaches, we introduced an anatomically precise head phantom containing a tumor mimic, enabling a more rigorous investigation of various FUS protocols for both partial and robotic-assisted complete tumor coverage under MRI monitoring. While previous studies mainly relied on thermometry to evaluate single lesion formation, this research shifts focus to high-resolution imaging for detailed visualization of both single and overlapping thermal lesions in tumor simulators. In addition, the FUS-induced thermal effects are compared between unobstructed sonication and sonication in the presence of 1-mm thick 3D-printed skull mimics. Importantly, the incorporation of robotic motion significantly enhances the simulation of clinical applications, providing a key benefit over earlier approaches.

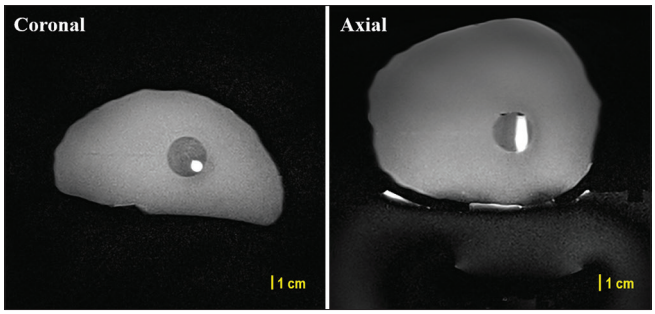

Figure 3: T2-weighted turbo spin echo images of the phantom showing the thermal lesion formed within the tumor from exposure at 105 W (5597 W/cm^2) for 30 s at a focal depth of 50 mm

In preclinical MRgFUS thermal therapy research, both agar-based and agar/PAA-based tumor phantom models have shown promise in evaluating ablation protocols and associated equipment.[13,14] Between the two, agar-based phantoms are advantageous due to their ease of preparation, handling, and overall ergonomics.[24] Nevertheless, a gap remains in the literature for simple, cost-effective TMPs that incorporate both anthropomorphic features and tumor simulators, particularly for evaluating MRgFUS applications in brain therapy.

Therefore, this study contributes to existing research by proposing a realistic tumor-bearing head phantom model and a reproducible method for simulating tumor ablation in MRgFUS thermal studies. The specific concentrations of phantom materials were informed by a previous study.[13] The

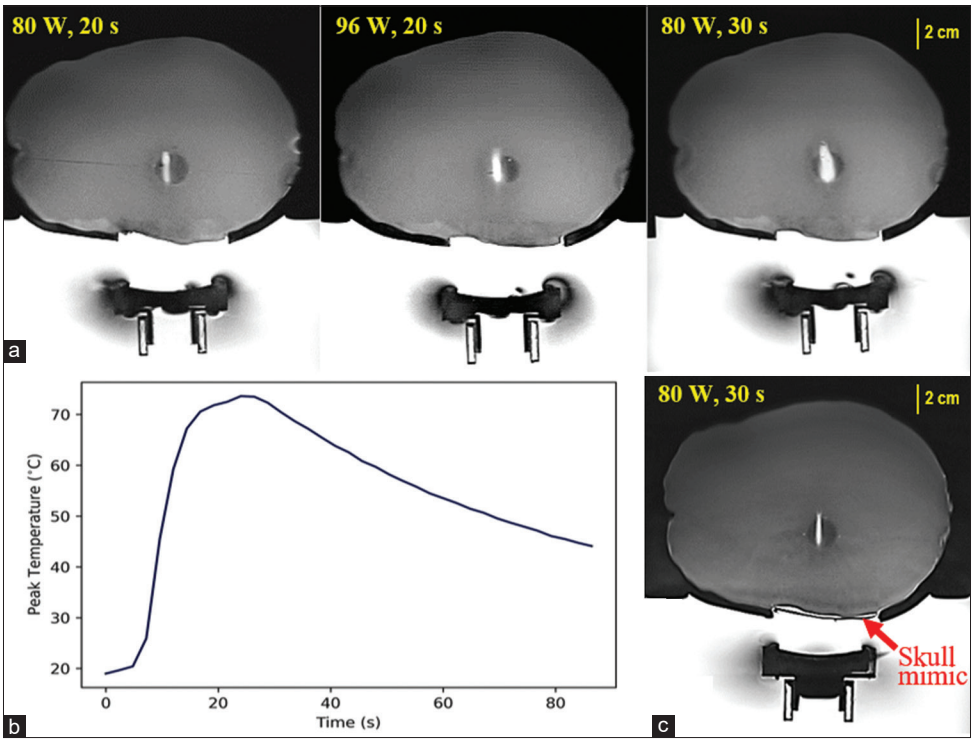

Figure 4: (a) T2-weighted turbo spin echo (T2-W TSE) images of the phantom after sonication of the tumor mimic at increasing acoustic energy levels (from left to right) without skull interference. (b) Focal temperature evolution recorded for the highest applied energy of 80 W for 30 s without a skull mimic. (c) T2-W TSE phantom image after tumor sonication at 80 W for 30 s through the resin skull

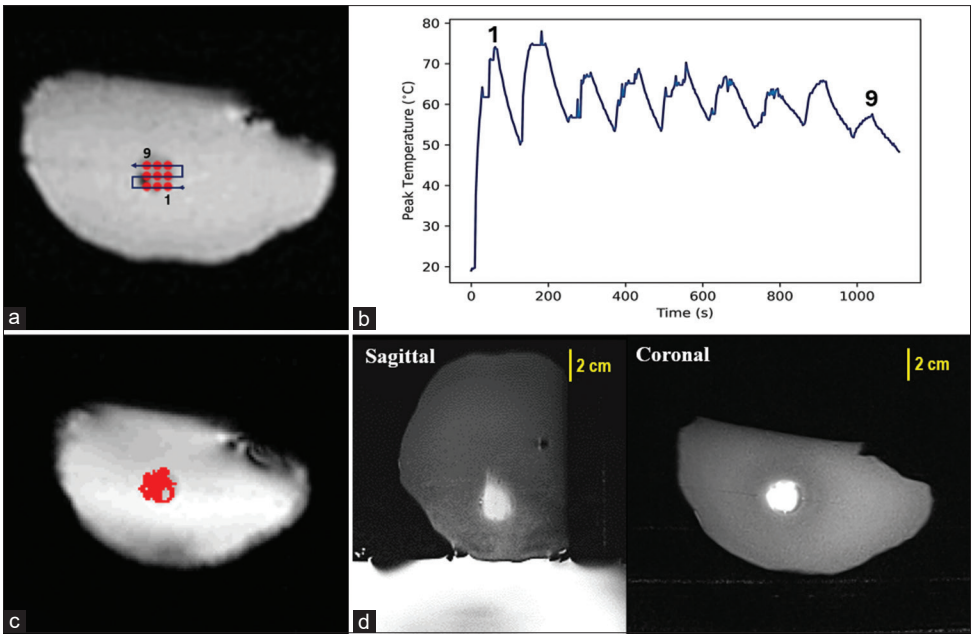

Figure 5: (a) Planned 3 × 3 sonication pattern (step of 5 mm) overlaid on fast low angle shot image of the phantom. (b) Timeseries of focal temperature evolution recorded at the nice sonication points, each exposed to 80 W (1838 W/cm2) for 60 s with a 60-s cooling time at a focal depth of 35 mm, without a skull mimic. (c) Corresponding simulated necrosis map. (d) Postsonication T2-weighted turbo spin echo phantom images revealing an overlapping lesion covering the entire tumor

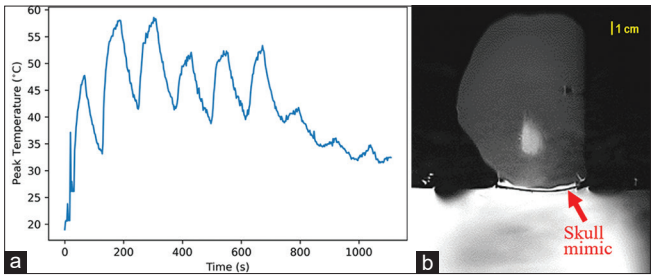

Figure 6: (a) Timeseries of focal temperature evolution recorded at the nice sonication points, each exposed to 80 W (1838 W/cm^2) for 60 s with a 60-s cooling time at a focal depth of 35 mm, through the 1-mm resin skull mimic. (b) Postsonication T2-weighted turbo spin echo sagittal phantom image revealing an overlapping lesion covering the entire tumor

current study confirmed that adding 4% w/v silica powder to a 6% w/v agar gel lowers signal intensity in T2-W TSE imaging by reducing effective water content, thus enabling clear delineation of the tumor mimic and effective sonication planning on the relevant software [Figure 1b].

High-power FUS produced distinct lesions in the tumor, visible as hyperintense regions on T2-W TSE images [Figure 3]. The increase in brightness upon heating is attributed to the disruption of the gel structure and water release, which is crucial for effective lesion monitoring. Notably, increasing the ultrasonic energy from 1600 to 2400 J resulted in a clear morphological change in the lesions, shifting from a thin, cigar-shaped form to a more pronounced egg shape [Figure 4]. Overlapping lesions were also created by robotic-assisted grid sonication, successfully covering the entire tumor [Figure 5].

The effect of 1-mm skull mimics, 3D-printed with three different polymers (Resin, ASA, and TPU), on FUS energy transmission and deposition in the tumor was investigated, primarily focusing on temperature changes at the focal spot [Table 2]. These results were compared to the unobstructed-field scenario, where no skull was present. The reasoning for exploring the implementation of a 1-mm skull mimic lies in the idea that temporarily excising a small section of the human skull and replacing it with a thin, biocompatible insert could enable FUS ablation of inoperable brain tumors using a simple single-element ultrasonic source. This approach would facilitate ablation by minimizing the intense beam aberration caused by variations in skull thickness, while leveraging the advantages of single-element transducers, such as their simplicity and cost-effectiveness compared to phased array transducers.

In the no-skull condition, the highest energy deposition occurred within the tumor mimic, as anticipated. A typical focal intensity of 1838 W/cm² applied for 30 s resulted in a temperature increase of 65.1°C at the focal spot. In the presence of the resin skull, a notable reduction in energy deposition was recorded, yet the temperature increase remained relatively high at 50.7°C, which is approximately 20% lower than the unobstructed-field condition. In contrast, ASA resulted in a limited temperature increase of 6.9°C, representing a 90% reduction compared to unobstructed sonication, indicating a significant obstruction in energy transmission. TPU, with the highest attenuation (23.1 ± 2.8 dB/cm-MHz according to prior literature), resulted in a minimal temperature rise of 2.3°C, reflecting a corresponding 96% reduction. These findings

also demonstrate a clear correlation between the ultrasonic attenuation properties of the materials and the reduction in focal temperature change [Table 2].

Further sonication experiments were conducted with the resin skull due to its demonstrated superior performance, confirming that its inclusion in the beam path results in approximately a 20% reduction in focal temperature increase compared to unobstructed-field conditions. Despite this reduction, sharp thermal lesions can still be effectively created, as shown in Figure 4c. The evaluation of grid sonications revealed a mean temperature of 68.1°C ± 5.5°C across the nine sonication points without a skull mimic, demonstrating consistent heating despite some variability from factors such as transducer energy fluctuations and recipe variations [Figure 5]. In contrast, sonication through the resin skull resulted in an average temperature of 48.4°C ± 8.2°C. The increased standard deviation observed indicates greater variability in temperature outcomes, suggesting that the skull mimic may introduce inconsistencies in energy deposition during grid sonication. Nevertheless, complete coverage of the tumor mimic was achieved, demonstrating accurate heating with no observable off-target effects [Figure 6].

A key consideration not addressed in this study is identifying a 3D printing resin material that meets the requirements for biocompatibility. While several biocompatible resins are available for 3D printing in medical applications,[25] their suitability for the proposed application requires further investigation. Therefore, future research will focus on evaluating these materials to assess their properties and determine their feasibility for this application. Future work could also explore the impact of increasing the resin skull mimic thickness to examine how 2-, 3-, and 4-mm barriers affect heat delivery and lesion formation. In addition, incorporating blood flow into the phantom could enhance simulation accuracy and provide more realistic insights into thermal dynamics during sonication.

Conclusions

This study utilized an anatomically accurate head phantom with an integrated tumor simulator to evaluate the effectiveness of various thermal protocols, with the ultimate goal of achieving complete tumor coverage. Two scenarios were tested: One without skull obstruction and the other with 1-mm thick polymer skull mimics intervening in the beam. High-resolution imaging with a T2-W TSE sequence effectively captured the thermal effects induced by FUS, providing direct visualization of both single and overlapping lesions as hyperintense (white) regions within the tumor model. Complete tumor coverage was achieved in both the unobstructed-field scenario and with the resin skull mimic present. The ASA and TPU skull mimics, characterized by higher attenuation coefficients, significantly hindered ultrasonic heating, leading to minimal temperature increases at the focal point. In contrast, the resin skull mimic allowed for efficient beam focusing and heating of the tumor to ablative levels, providing preliminary evidence for the potential application of a thin biocompatible implant to temporarily replace a portion of the skull, facilitating the ablation of inoperable tumors using a single-element concave transducer. This approach aims to address the challenges associated with MRgFUS ablation of brain tumors through the human skull, which is currently not feasible. The employed phantom could serve as a valuable tool for further examining the feasibility of this application, as well as for calibrating MRgFUS systems and validating thermal therapy plans in oncology.

Acknowledgment

Furthermore, we would like to express our sincere gratitude to Dr. Samuel Pichardo for providing the MR thermometry code, which was integrated into the MRgFUS software used in this study.

Financial support and sponsorship

The study was funded by the Recovery and Resilience Facility of the NextGenerationEU instrument, through the Research and Innovation Foundation (RIF) of Cyprus, under the projects BRAINSONIC (ENTERPRISES/0223/Sub-Call1/0057) and FUSVET (SEED/1221/0080).

Conflicts of interest

There are no conflicts of interest.

References

1. Dabbagh A, Abdullah BJ, Ramasindarum C, Abu Kasim NH. Tissue-mimicking gel phantoms for thermal therapy studies. Ultrason Imaging 2014;36:291-316.
2. McGarry CK, Grattan LJ, Ivory AM, Leek F, Liney GP, Liu Y, *et al.* Tissue mimicking materials for imaging and therapy phantoms: A review. Phys Med Biol 2020;65(23). [doi: 10.1088/1361-6560/abbd17].
3. Haemmerich D, Schutt DJ. RF ablation at low frequencies for targeted tumor heating: *In vitro* and computational modeling results. IEEE Trans Biomed Eng 2011;58:404-10.
4. Zhong X, Zhou P, Zhao Y, Liu W, Zhang X. A novel tissue-mimicking phantom for US/CT/MR-guided tumor puncture and thermal ablation. Int J Hyperthermia 2022;39:557-63.
5. Zhou Y, Zhao L, Zhong X, Ding J, Zhou H, Wang F, *et al*. A thermochromic tissue-mimicking phantom model for verification of ablation plans in thermal ablation. Ann Transl Med 2021;9:354.
6. Ortega-Palacios R, Trujillo-Romero CJ, Cepeda-Rubio MF, Leija L, Vera Hernández A. Heat transfer study in breast tumor phantom during microwave ablation: Modeling and experimental results for three different antennas. Electronics (Basel) 2020;9:535.
7. Liu Z, Ahmed M, Weinstein Y, Yi M, Mahajan RL, Goldberg SN. Characterization of the RF ablation-induced 'oven effect': The importance of background tissue thermal conductivity on tissue heating. Int J Hyperthermia 2006;22:327-42.
8. Kim KS, Lee SY. Nanoparticle-mediated radiofrequency capacitive hyperthermia: A phantom study with magnetic resonance thermometry. Int J Hyperthermia 2015;31:831-9.
9. Kaczmarek K, Hornowski T, Antal I, Rajnak M, Timko M, Józefczak A. Sono-magnetic heating in tumor phantom. J Magn Magn Mater 2020;500:166396.
10. Damianou C. The role of phantoms in magnetic resonance imaging-guided focused ultrasound surgery. Digit Med 2019;5:52-5.
11. Menikou G, Dadakova T, Pavlina M, Bock M, Damianou C. MRI compatible head phantom for ultrasound surgery. Ultrasonics 2015;57:144-52.

12. Antoniou A, Nikolaou A, Georgiou A, Evripidou N, Damianou C. Development of an US, MRI, and CT imaging compatible realistic mouse phantom for thermal ablation and focused ultrasound evaluation. Ultrasonics 2023;131:106955.
13. Antoniou A, Evripidou N, Georgiou L, Chrysanthou A, Ioannides C, Damianou C. Tumor phantom model for MRI-guided focused ultrasound ablation studies. Med Phys 2023;50:5956-68.
14. Sofokleous P, Damianou C. High-quality agar and polyacrylamide tumor-mimicking phantom models for magnetic resonance-guided focused ultrasound applications. J Med Ultrasound 2024;32:121-33.
15. Antoniou A, Evripidou N, Damianou C. Focused ultrasound heating in brain tissue/skull phantoms with 1 MHz single-element transducer. J Ultrasound 2024;27:263-74.
16. Drakos T, Antoniou A, Evripidou N, Alecou T, Giannakou M, Menikou G, *et al.* Ultrasonic attenuation of an agar, silicon dioxide, and evaporated milk gel phantom. J Med Ultrasound 2021;29:239-49.
17. Drakos T, Giannakou M, Menikou G, Constantinides G, Damianou C. Characterization of a soft tissue-mimicking agar/wood powder material for MRgFUS applications. Ultrasonics 2021;113:106357.
18. Drakos TM, Menikou G, Filippou A, Evripidou N, Spanoudes K, Ioannou L, *et al*. MRI-guided focused ultrasound robotic system for preclinical use. J Vet Med Anim Sci 2020;4:1049.
19. Filippou A, Georgiou A, Nikolaou A, Evripidou N, Damianou C. Advanced software for MRgFUS treatment planning. Comput Methods Programs Biomed 2023;240:107726.
20. Kuroda K. MR techniques for guiding high-intensity focused ultrasound (HIFU) treatments. J Magn Reson Imaging 2018;47:316-31.
21. Rieke V, Butts Pauly K. MR thermometry. J Magn Reson Imaging 2008;27:376-90.
22. Antoniou A, Evripidou N, Giannakou M, Constantinides G, Damianou C. Acoustical properties of 3D printed thermoplastics. J Acoust Soc Am 2021;149:2854.
23. Antoniou A, Damianou C. Feasibility of ultrasonic heating through skull phantom using single-element transducer. J Med Ultrasound 2024;32:32-40.
24. Antoniou A, Damianou C. MR relaxation properties of tissue-mimicking phantoms. Ultrasonics 2022;119:106600.
25. Guttridge C, Shannon A, O'Sullivan A, O'Sullivan KJ, O'Sullivan LW. Biocompatible 3D printing resins for medical applications: A review of marketed intended use, biocompatibility certification, and post-processing guidance. Ann 3D Print Med 2022;5:100044.